Mössbauer Effect in Magnetic Thin Films: Recent Results and Perspectives

Dénes Lajos Nagy

KFKI Research Institute for Particle and Nuclear Physics, Budapest, Hungary

50 Years After - the Mössbauer Effect Today and in Future

TU München, Physics-Department, Garching, 9-10 October 2008

Outline

- Motivation: examples presenting the state-of-art of Mössbauer effect methodology in magnetic thin film studies
- Brief overview of relevant Mössbauer techniques (CEMS, GIMS, MES, NRS)
- Arbitrarily chosen methodological highlights of the past decade
- Two topics in somewhat more detail:
  - Orientation of the layer magnetisation
  - Domain structure of coupled multilayers
- Outlook

Magnetic thin films: applications

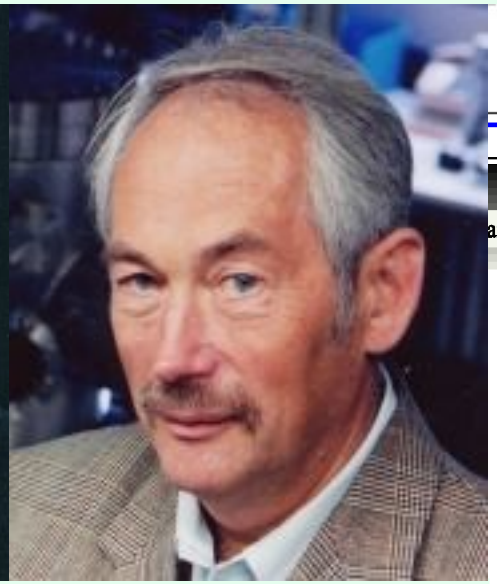

A. Fert and P. Grünberg
Nobel Prize in physics, 2007

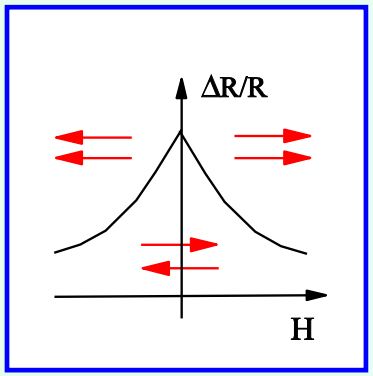

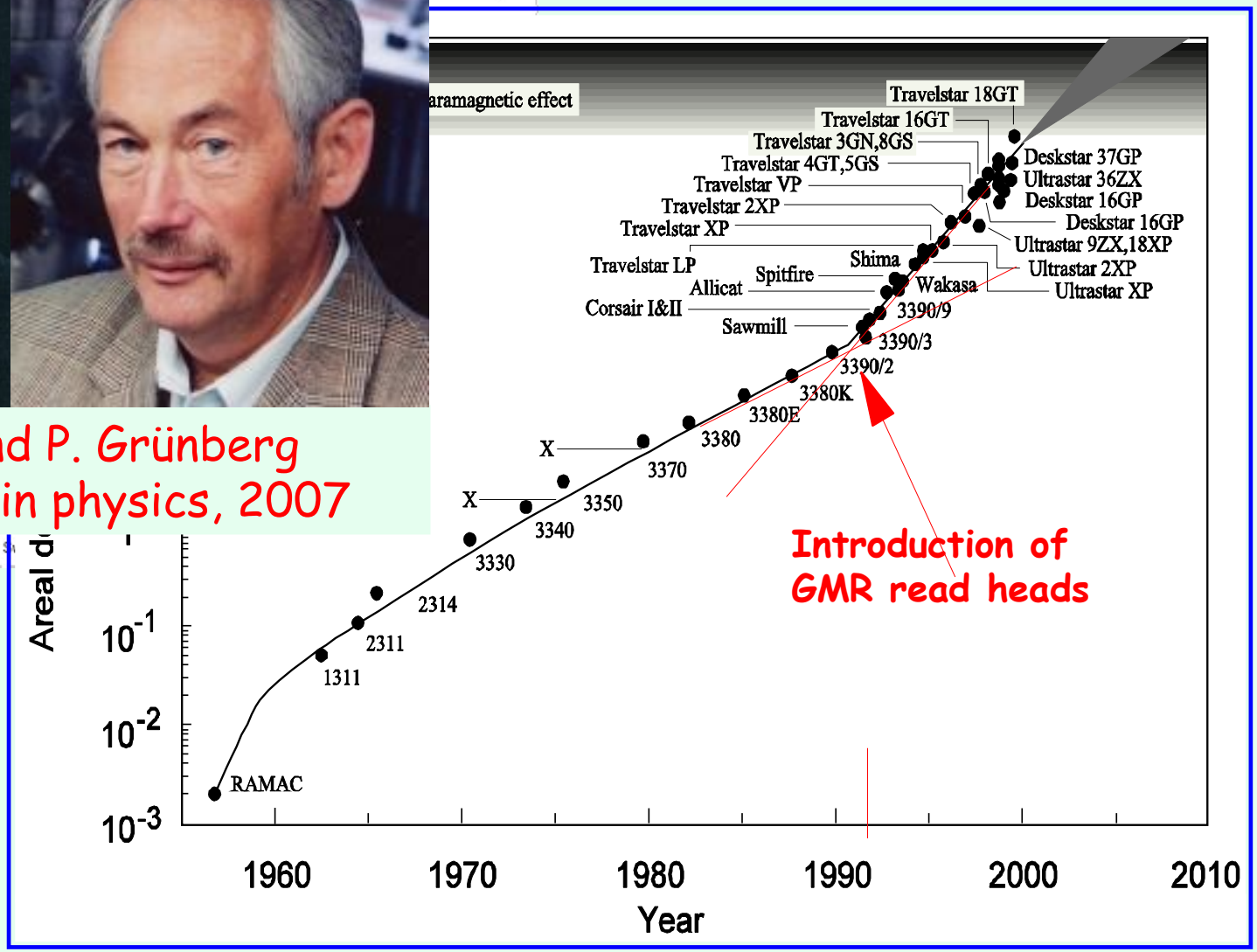

Some properties affecting the performance of GMR devices

Property	Mössbauer parameters	Mössbauer methods
Chemical composition of layers and interfaces	Hyperfine parameters	Phase analysis: transmission, CEMS, emission, NRS
Orientation of layer and interface magnetisation	Angular distribution and polarisation of resonant transitions: line intensities and beating depths	Mössbauer polarimetry, CEMS polarimetry, NR magnetometry, NR polarimetry
Superparamagnetism Diffusion	Distortion of the shape of energy- and time-domain spectra	Mössbauer transmission, CEMS, NRS
Magnetic domain structure, magnetic roughness	Width (shape) of the diffuse nuclear resonant scatter	Off-specular synchrotron Mössbauer reflectometry
Lattice vibrations in layers, surfaces and interfaces	Intensity of nuclear resonant inelastic scattering vs. energy	Nuclear resonant inelastic scattering

Mössbauer techniques for magnetic thin film studies

Technique	Advantages	Drawbacks
Transmission and nuclear resonant forward scattering	Simple arrangement, wide possibilities for sample environments	High absorption by the substrate
CEMS and DCEMS (gas-flow counter)	Inherent thin-film sensitivity, high efficiency	Poor depth resolution of DCEMS, limitations for sample environment, not applicable in vacuo
CEMS and DCEMS (channeltron or microchannel plate)	Inherent thin-film sensitivity, good depth resolution of DCEMS, applicable in UHV	Low efficiency, limitations for sample environment
GIMS (laboratory sources)	Inherent thin-film sensitivity, excellent depth resolution	Very low efficiency, limitations for sample environment, not applicable in vacuo

Te

Emission

Grazing-in
resonar
synchrot
refle

Nuclear re
sc

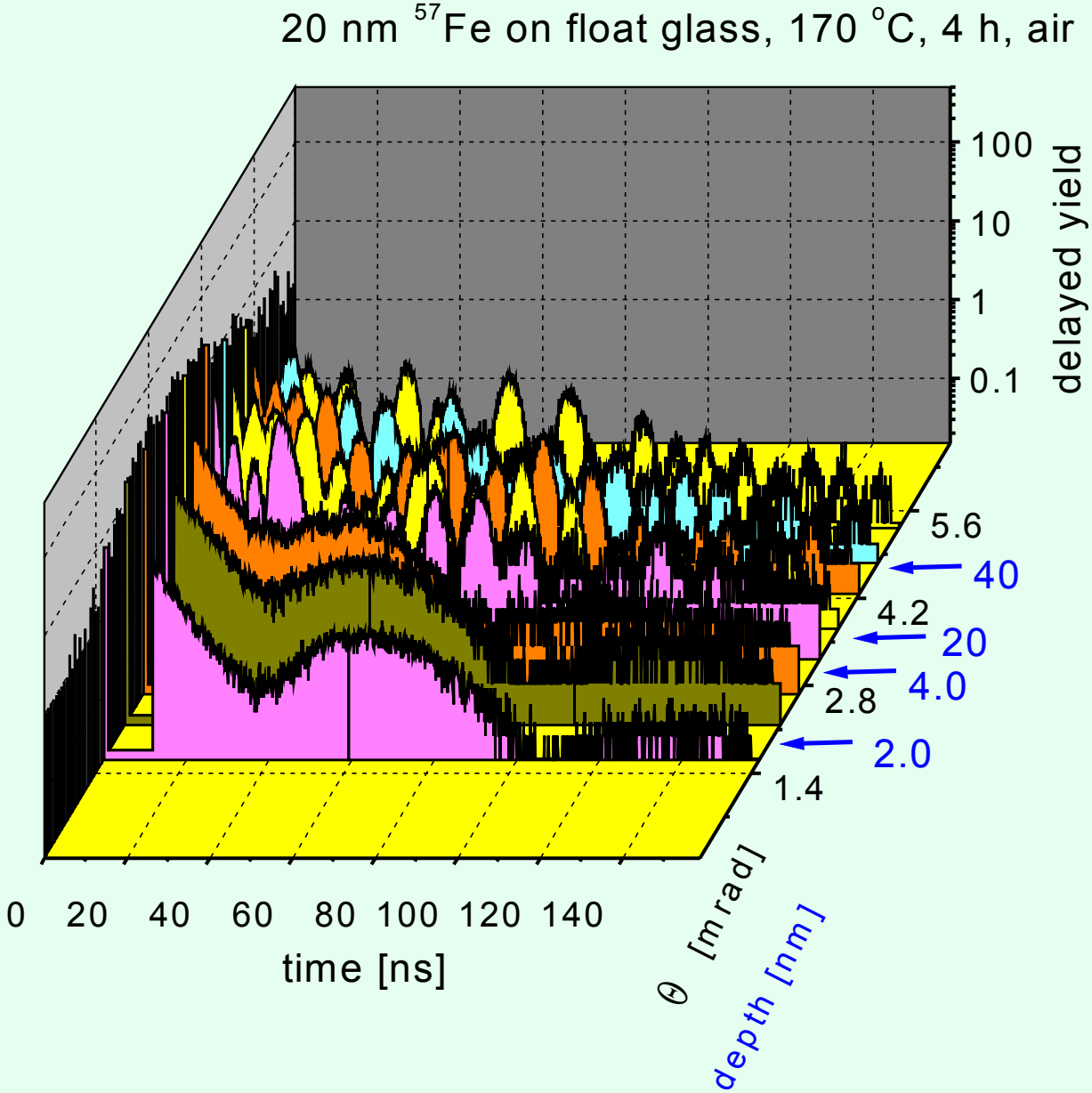

ks

n sample
nitations
ronment

otron
ssibly
-situ UHV
ation is

otron
ssibly
-situ UHV
ation is

Mössbauer holography

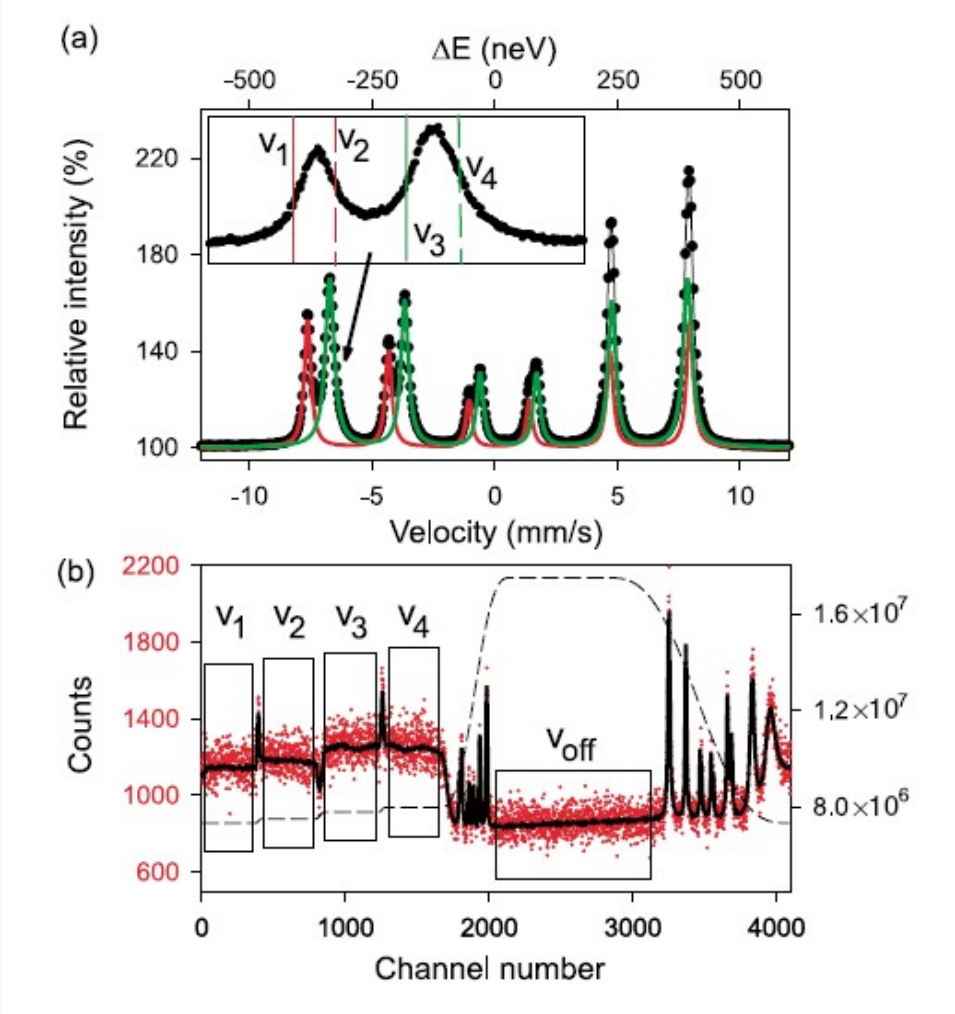

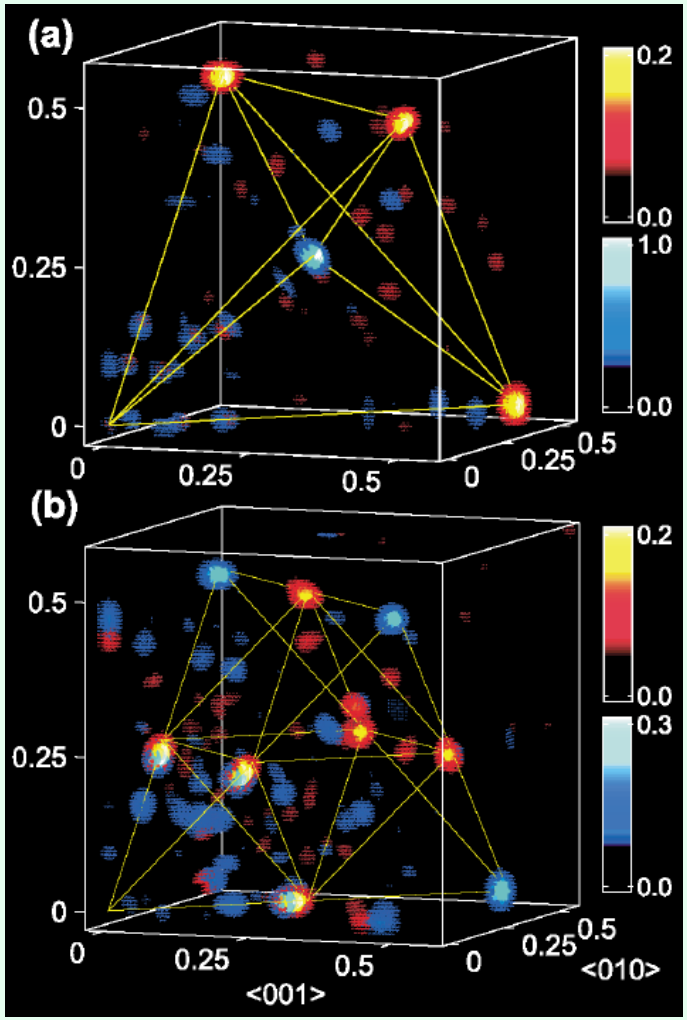

α-Fe thin film: P. Korecki et al., Fe_3O_4 thin film: PRL **79**, 3518 (1997), P. Korecki et al., PRL **92**, 205501 (2004)

ILEEMS

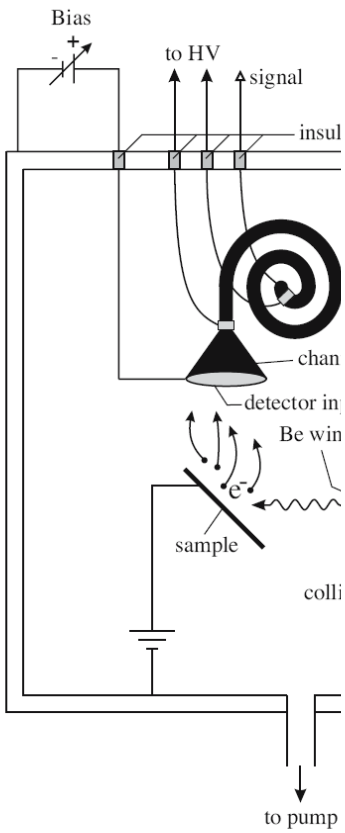

Figure 2. Sketch of the measur

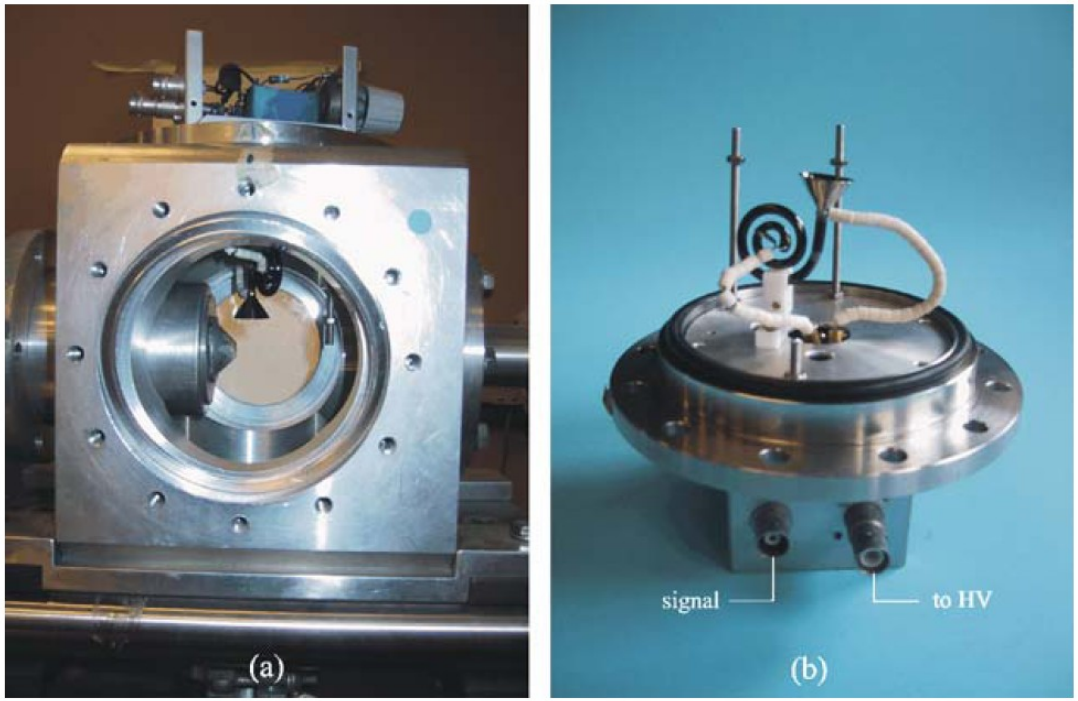

Figure 3. (a) View of the inside of the ILEEMS measuring chamber from the entry port for the cryostat. On the left is the cone with Be window for the incident radiation. The channeltron is closely above it. On top of the cubic chamber on the outside is the voltage divider. (b) Picture of disassembled top plate showing the mounting of the channeltron.

Integral low-energy electron Mössbauer spectroscopy, ILEEMS (E. de Grave et al., Hyp. Int. **161**, 147 (2005)): detecting low-energy (15 eV) electrons using a biased channeltron. Information depth: a few nm.

UHV chamber for in-situ NRS studies of surface nanostructures at ESRF ID18

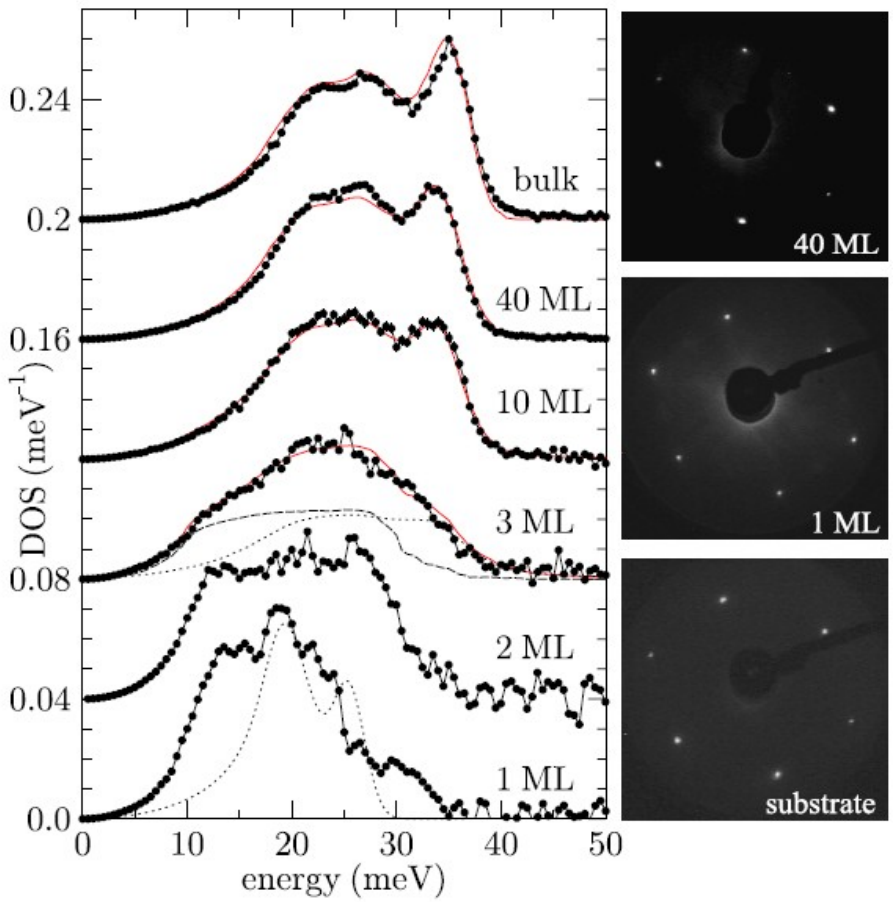

FIG. 1 (color online). DOS of single-crystalline Fe films on W(110) for thicknesses ranging from the monolayer to a 40 ML thick film (thickness equivalent: 1 ML ≡ 0.2 nm). For clarity, the curves are displaced from another by 0.04 meV^{-1}. The solid line in the upper graph represents the density of phonon states of polycrystalline bulk α-iron, i.e., the ambient temperature bcc phase of iron [24] as calculated from neutron data and convoluted with the energy resolution function of this experiment. The dashed and dotted line in the DOS of the 3 ML film represent the smoothed DOS of the 2 ML film and the DOS of bulk bcc Fe convoluted with a damped harmonic oscillator (quality factor $Q = 7$), respectively, out of which the DOS of the 3 ML film seems to be composed of. The solid lines for the 3, 10, and 40 ML DOS result from the weighted sum of these two contributions in each case. The dotted line in the lower graph represents the phonon DOS of bulk bcc W for comparison. The right column shows LEED patterns ($E = 96$ eV) of the bare substrate, 1 and 40 ML films recorded right after preparation of the films.

S. Stankov et al., PRL **99**, 185501 (2007)

European Community FP6 Specific Targeted Research Project
Contract No. NMP4-CT-2003-001516 (DYNASYNC)

In-situ Mössbauer emission spectroscopy of electrodeposited magnetic thin films

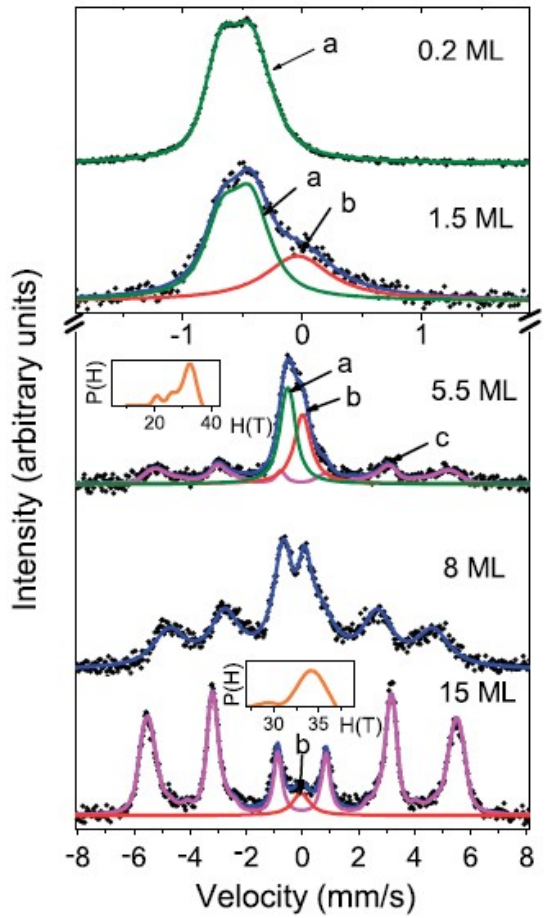

Fig. 2. Mössbauer spectra of ^{57}Co deposited on Ag(100). a: Separate, b: clustered, c: magnetically ordered (^{57}Co)^{57}Fe atoms.

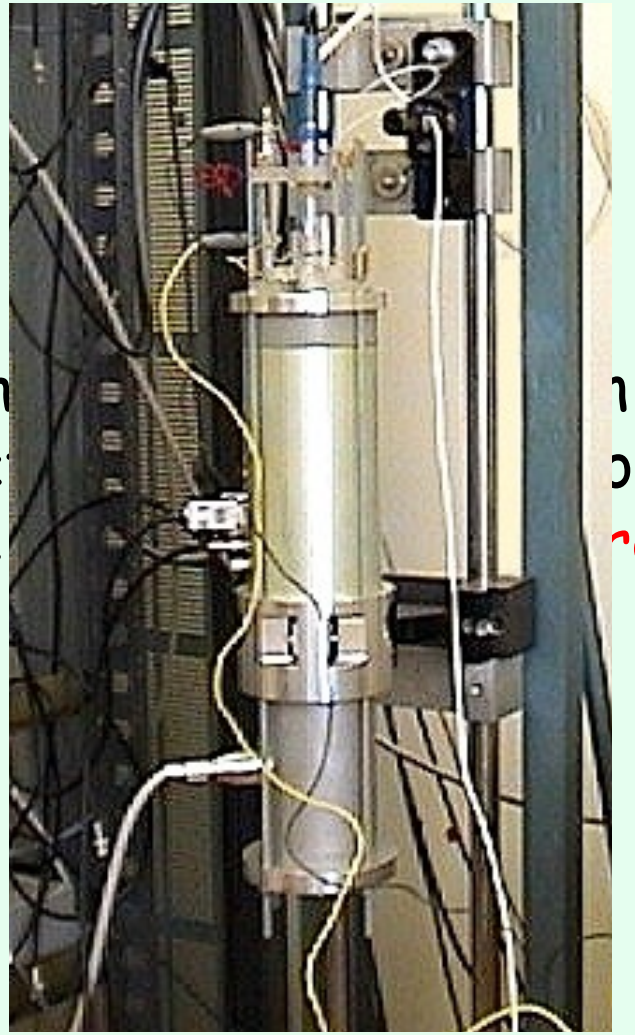

Th n the
elec only to
the round!

I. Dézsi, Cs. Fetzer, Electrochem. Commun. 9, 1846 (2007)

Polarised photons

- Linearly polarised photons may only see the alignment of $\mathbf{H}_{hf}$.

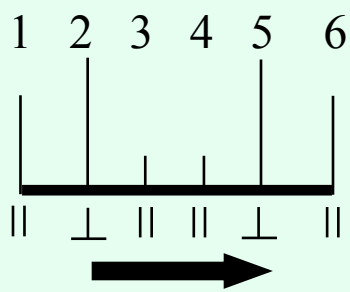

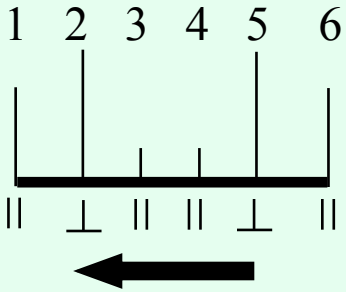

- Circularly polarised photons may also see the sign of $\mathbf{H}_{hf}$ — possibility for measuring the direction.

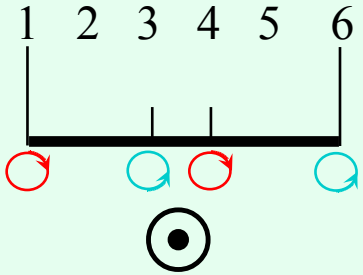

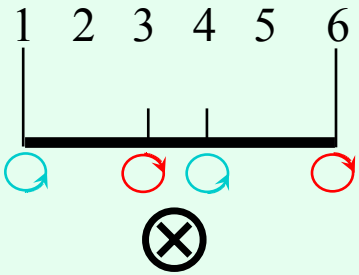

Linear CEMS polarimetry using an in-plane magnetised $^{57}Co(\alpha\text{-}Fe)$ source

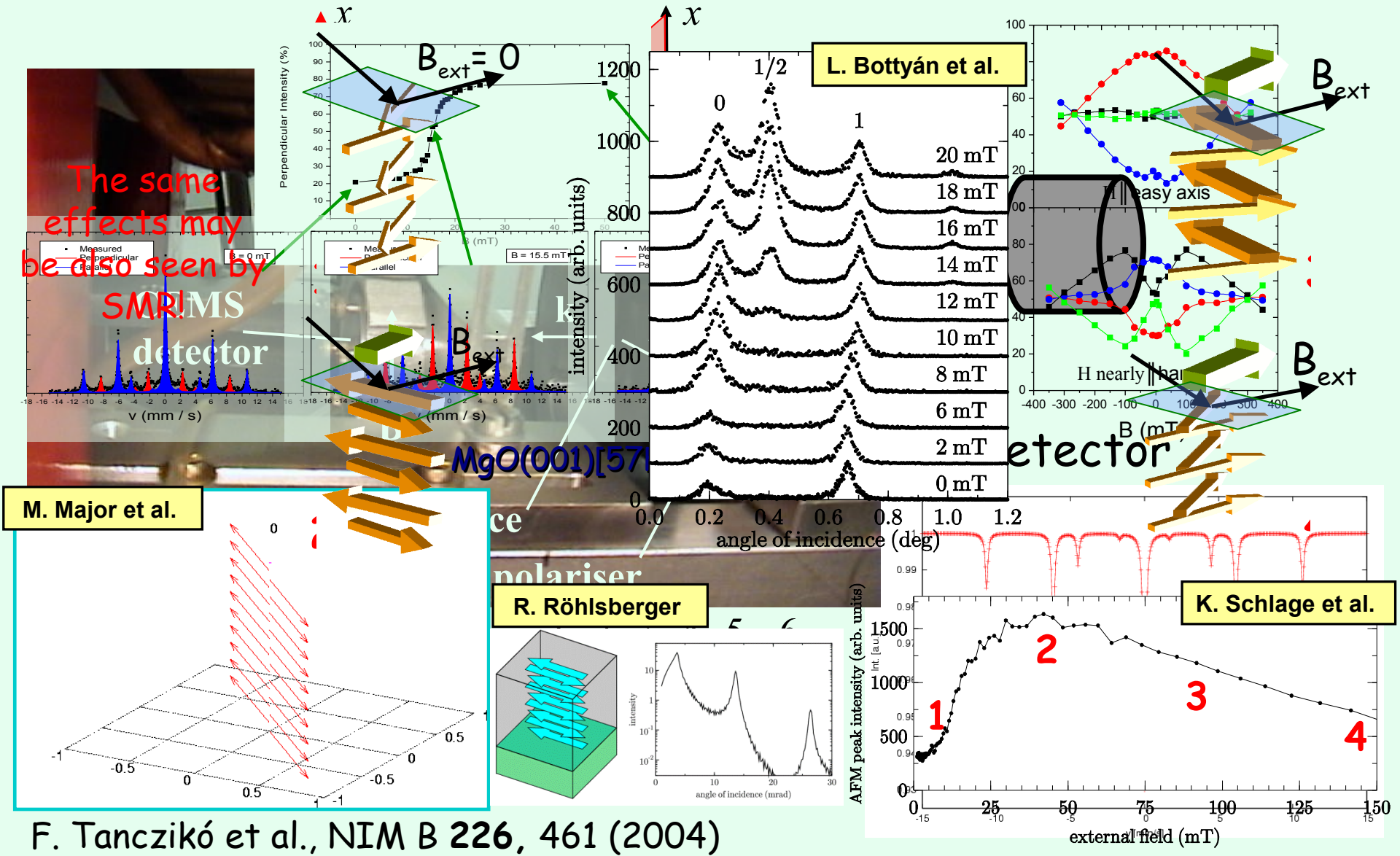

F. Tanczikó et al., NIM B **226**, 461 (2004)

Circular (elliptic) CEMS polarimetry

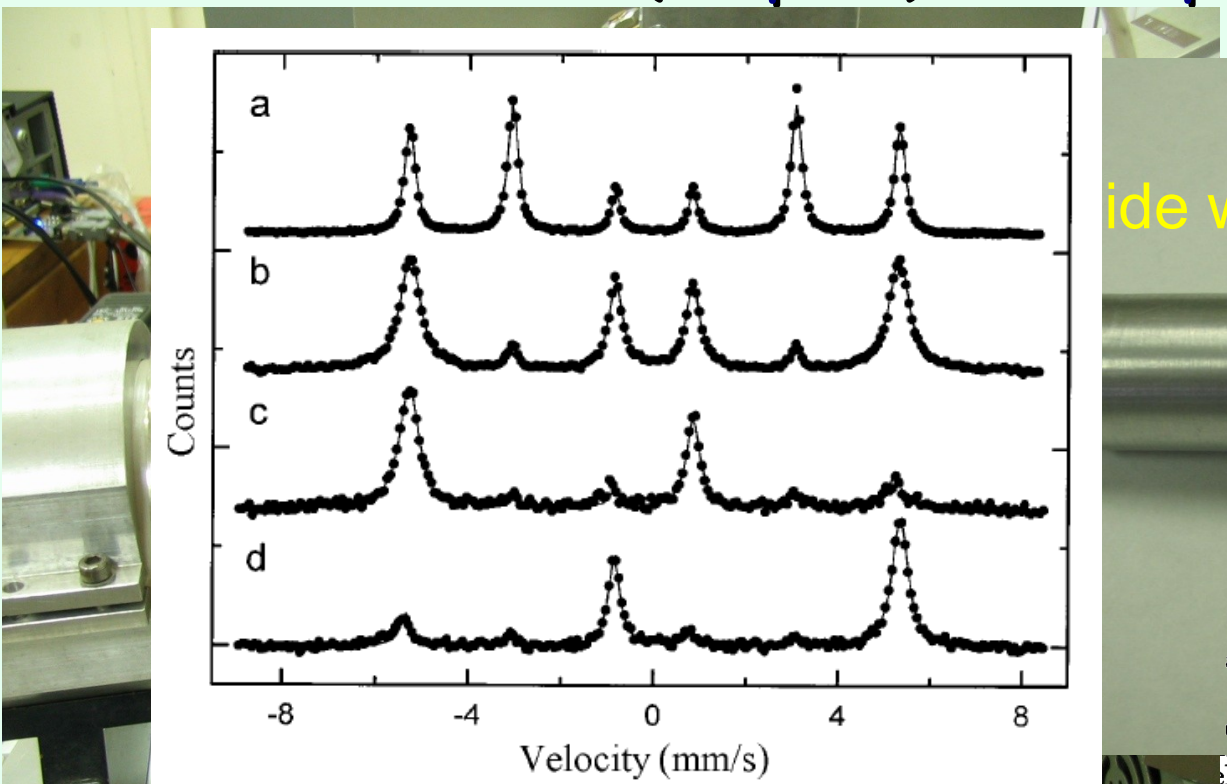

Fig. 1. The CEMS spectrum of α-^{57}Fe measured with unpolarized beam when ***k*** vector is (a) perpendicular and (b) almost parallel to external magnetic field and sample plane. The same sample measured with circularly polarized radiation when ***k*** vector is almost (c) parallel and (d) antiparallel to the external magnetic field.

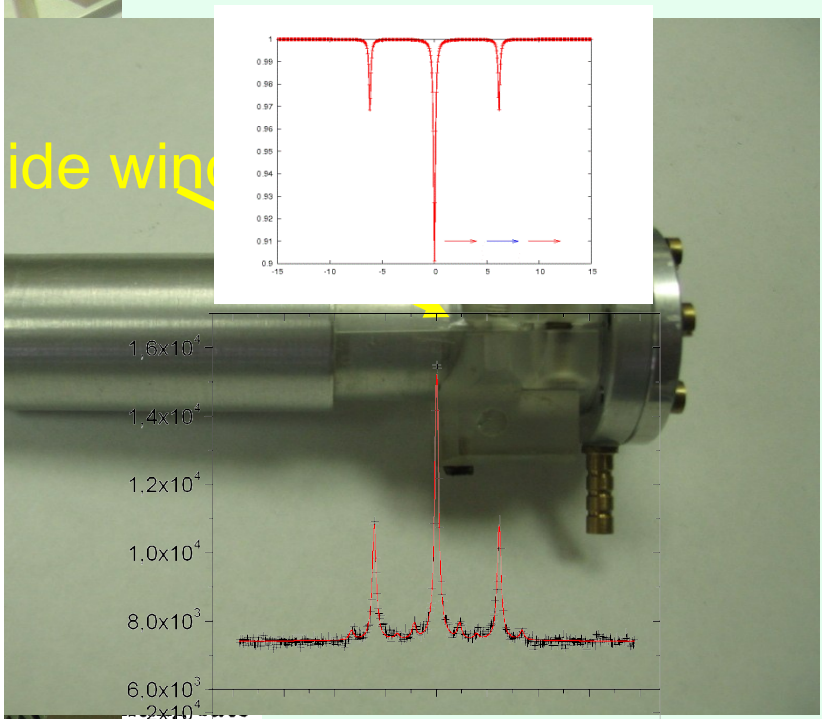

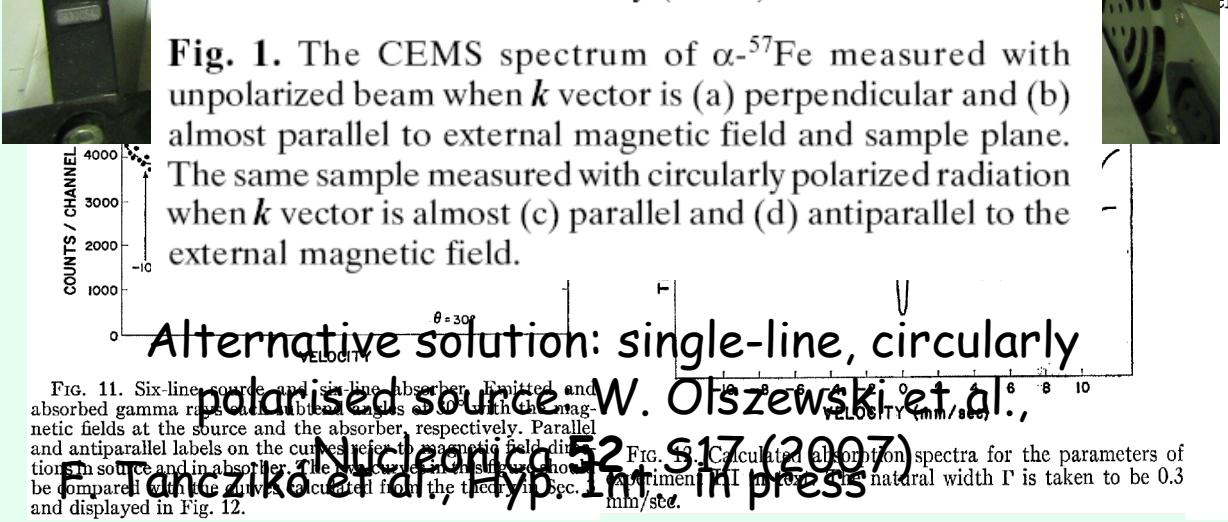

FIG. 11. Six-line source and six-line absorber. Emitted and absorbed gamma rays each subtend angles of 30° with the magnetic fields at the source and the absorber, respectively. Parallel and antiparallel labels on the curves refer to magnetic field directions in source and in absorber. The spectra in this figure should be compared with the curves calculated from the theory in Sec. 12 and displayed in Fig. 12.

FIG. 13. Calculated absorption spectra for the parameters of experiment VII under the natural width Γ is taken to be 0.3 mm/sec.

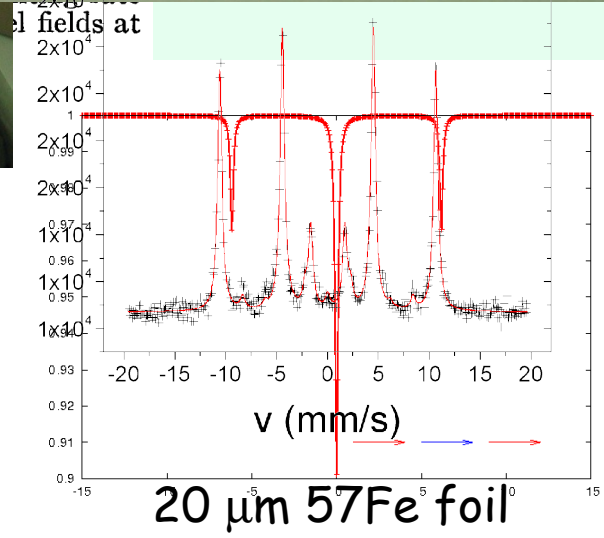

20 μm 57Fe foil

Alternative solution: single-line, circularly polarised source. W. Olszewski et al., Hyperfine Interactions 52, 317 (2007) and Kobeissi et al., pp. 111, in press

Circular (elliptic) polarimetry by NRS

160 nm ^{57}Fe film on mica

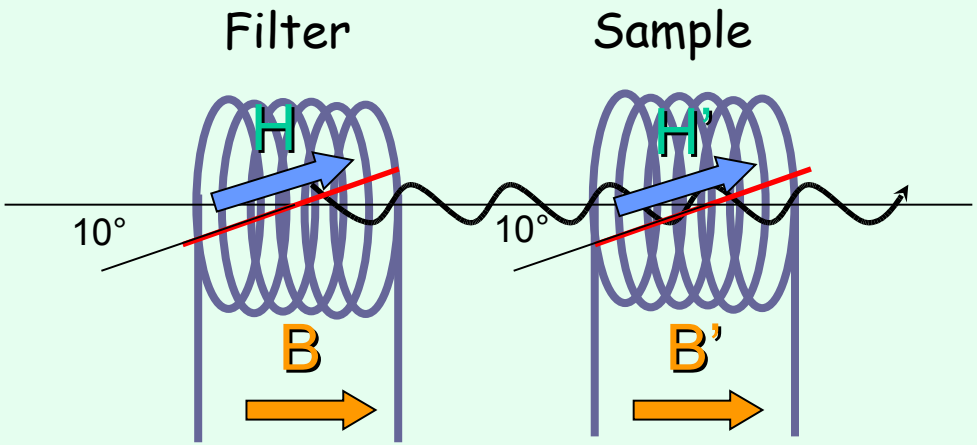

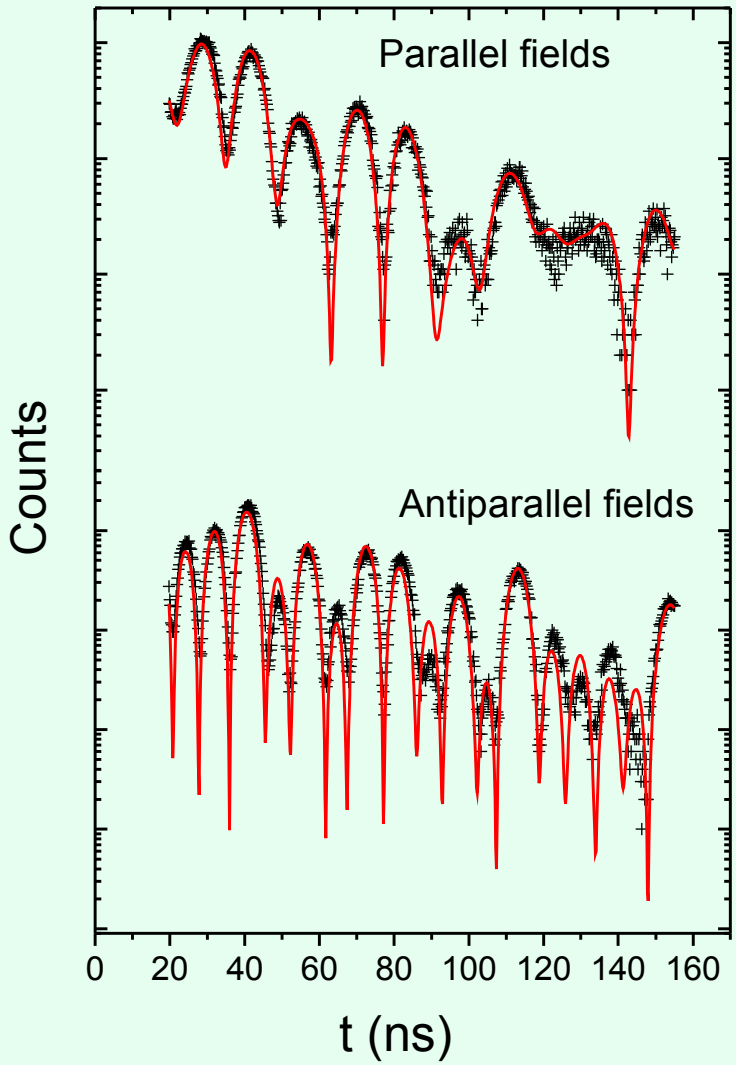

F. Tanczikó et al., to be published

ESRF ID18

Nuclear resonant magnetometry using λ/4 phase-retarder plate and constant-velocity single-line reference

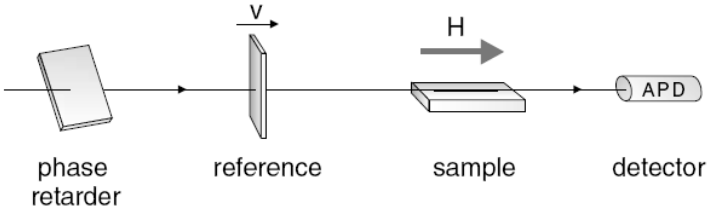

FIG. 2. Setup for nuclear resonant magnetometry.

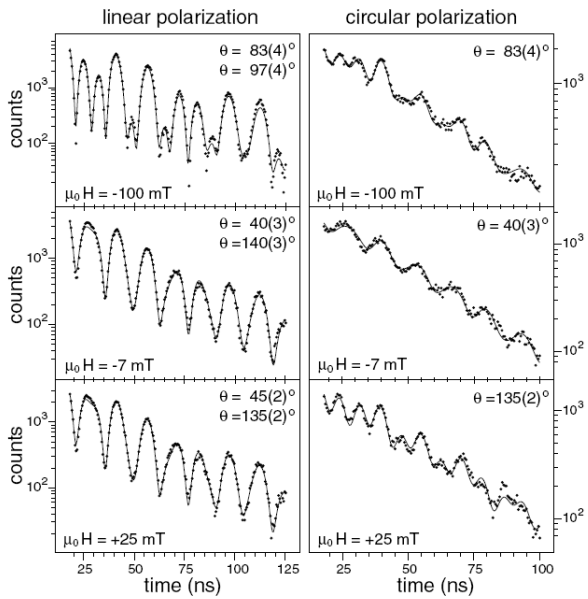

FIG. 3. Experimental time spectra for different external field values taken with linearly polarized radiation (left) and circularly polarized radiation (right). The line represents the theoretical fit to the data. θ is the in-plane angle between $\vec{M}$ and $\vec{k}$ obtained from the fit.

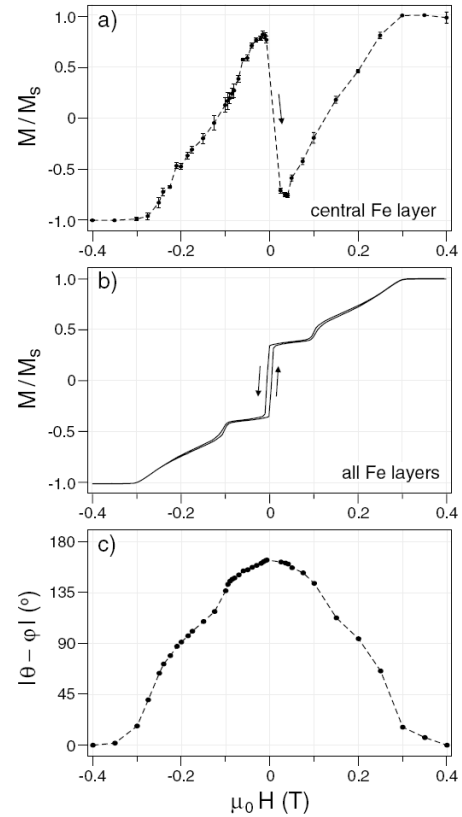

FIG. 4. Magnetization measurements with the applied field along one of the easy axes in the sample. (a) Magnetization curve obtained via nuclear resonant magnetometry. (b) Macroscopic magnetization curve. (c) Angle between the magnetization vectors in the central and the outer Fe layers obtained from the curves (a) and (b) as explained in the text.

^{56}Fe(50 Å)/Cr(11 Å)/^{57}Fe(50 Å)/Cr(11 Å)/^{56}Fe(50 Å)

L'abbé et al., PRL **93**, 037201 (2004)

Magnetometry by circular CEMS polarimetry

AF-coupled asymmetric Fe/Cr trilayer

Fe(20 nm)/Cr(1.2 nm)/^{57}Fe(5 nm)/Cr(2.4 nm)

After field reversal, in remanence

Spin-flop

Magnetisation reversal

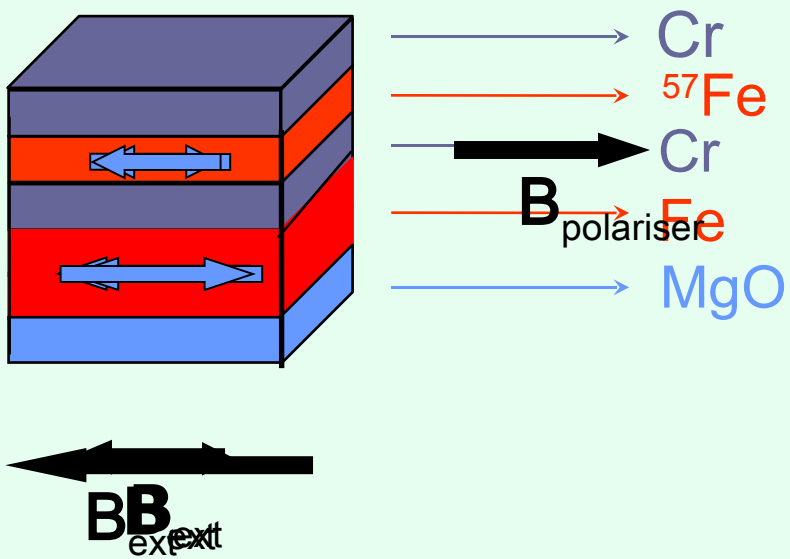

Remanence

B_{ext} = 400 mT

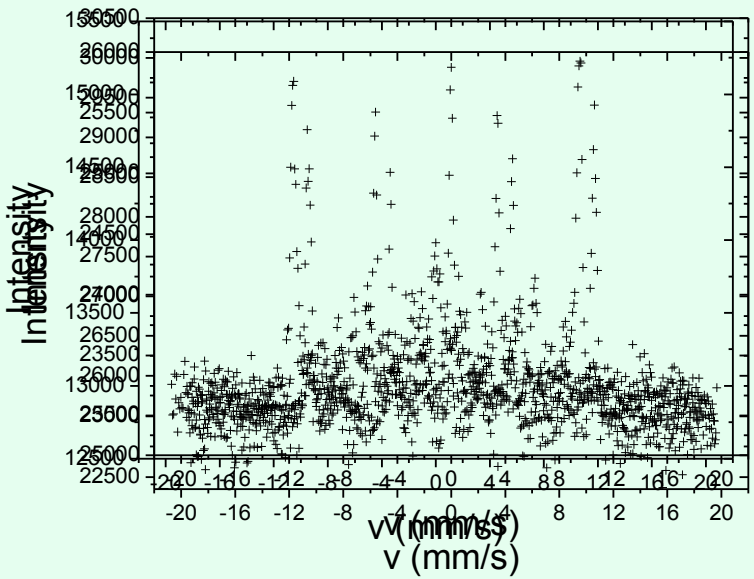

F. Tanczikó et al., to be published

Patch domains in AF-coupled multilayers

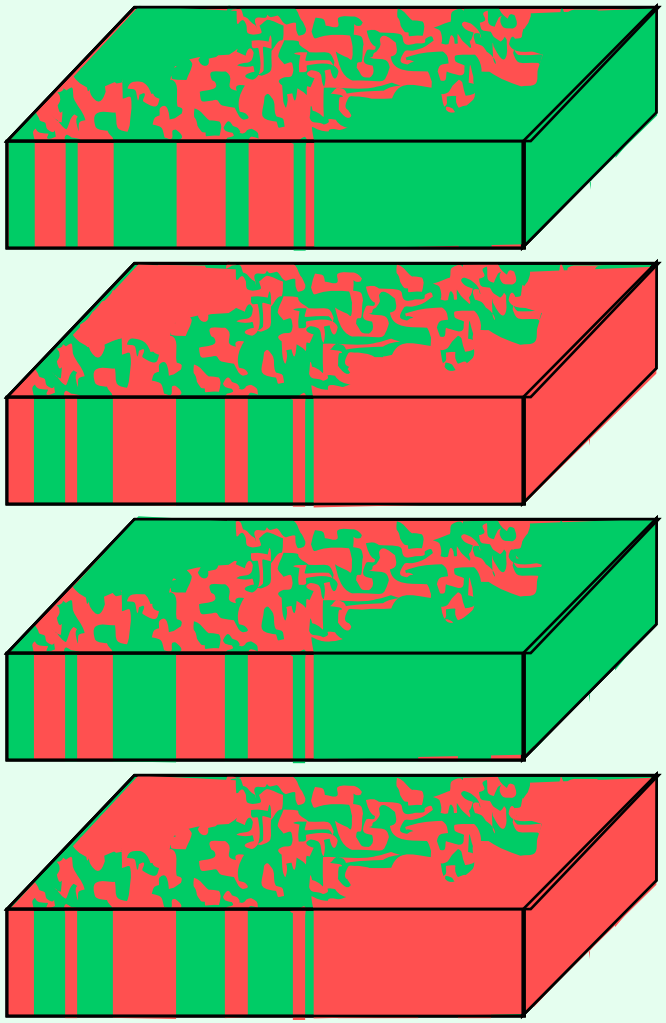

Layer magnetisations:

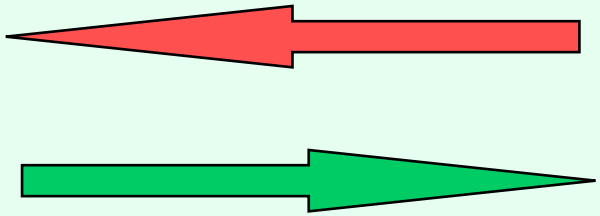

The 'magnetic field lines' are shortcut by the AF structure → the stray field is reduced → no 'ripple' but 'patch' domains are formed.

Arrangement of an SMR experiment

from the high-resolution monochromator

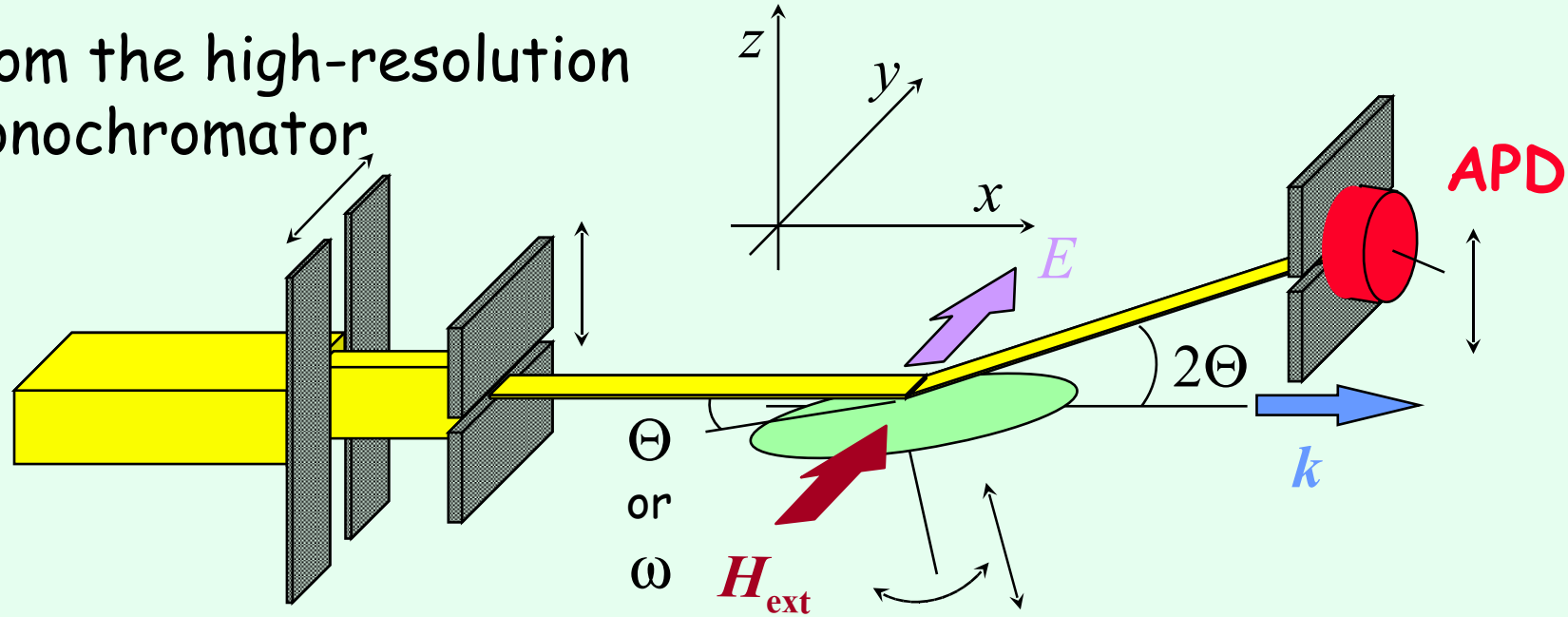

$\Theta/2\Theta$ scan: Q_x scan

ω scan: Q_z scan

$$\xi = \frac{d}{\Delta Q_x} = \frac{2\pi}{\Delta Q_z}$$

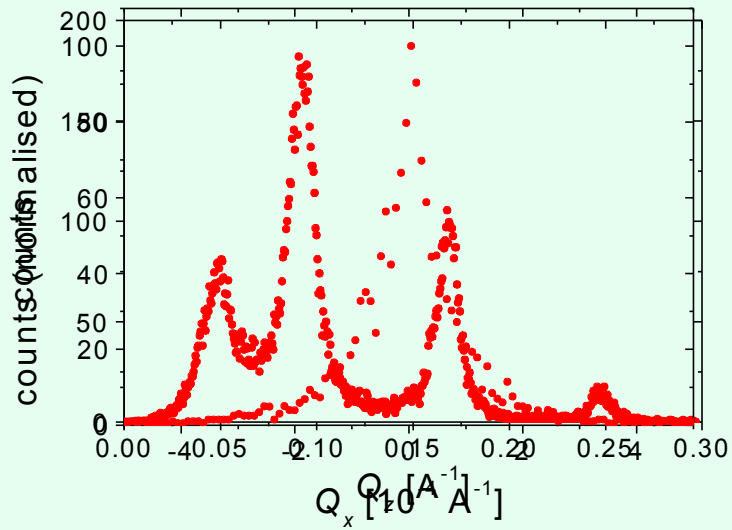

Domain ripening: off-specular SMR

MgO(001)[^{57}Fe(26Å)/Cr(13Å)]$_{20}$
2Θ @ AF reflection, hard axis

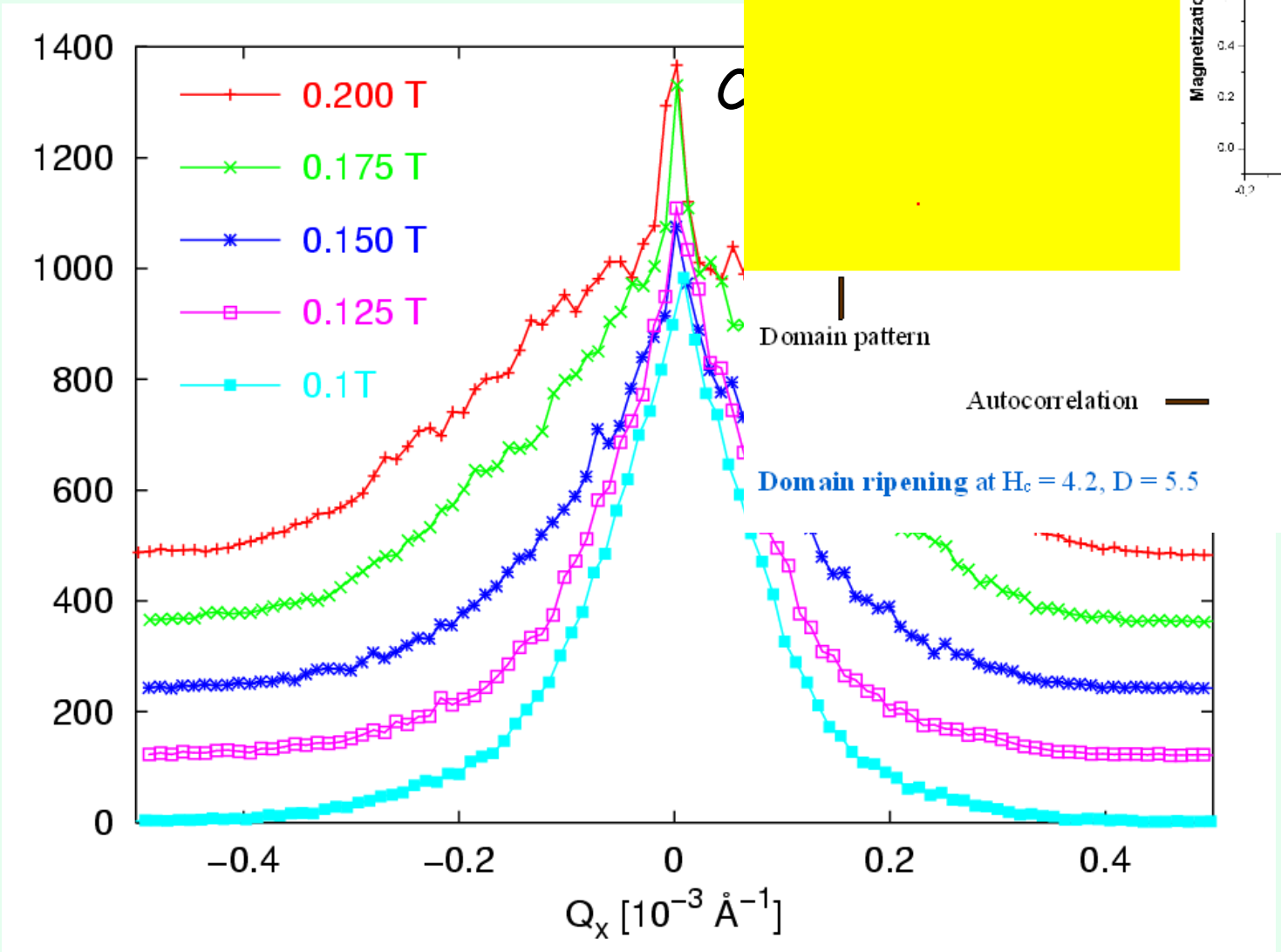

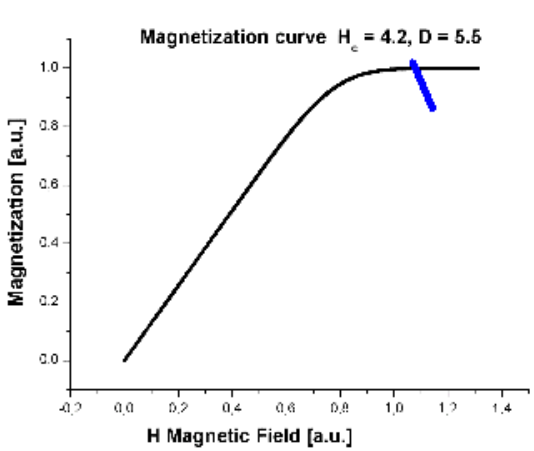

ESRF
ID18

Spin-flop-induced domain coarsening (SMR)

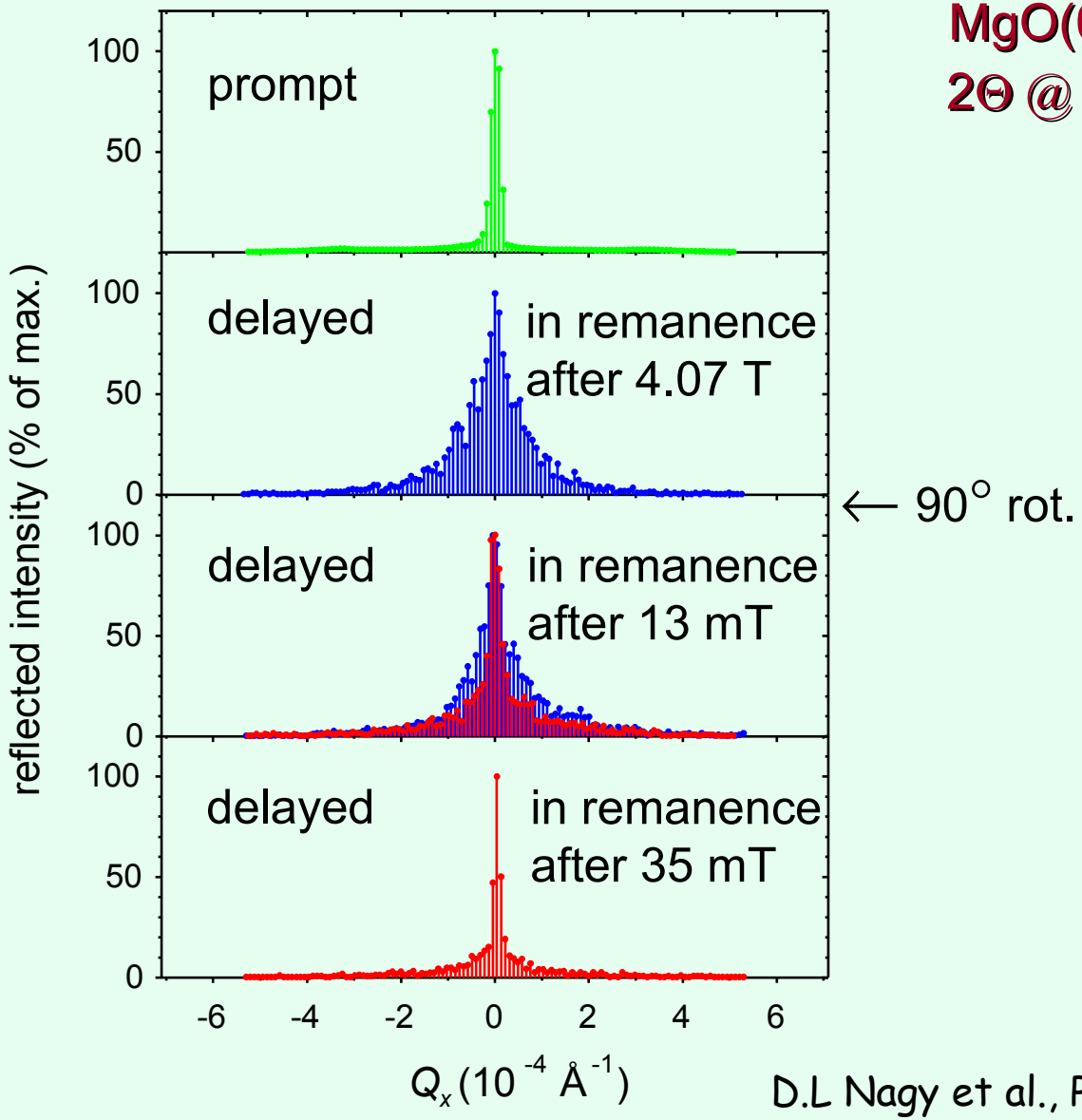

MgO(001)[^{57}Fe(26Å)/Cr(13Å)]$_{20}$

2Θ @ AF reflection, easy axis

Correlation length:

$$\xi = 1/\Delta Q_x$$

Delayed photons before the spin flop

$\xi = 800$ nm

Delayed photons after the spin flop

$\xi_1 > 5$ μm

$\xi_2 = 800$ nm

D.L Nagy et al., PRL **88**, 157202 (2002)

ESRF ID18

2D SMR: APD array and simplified DWBA

$MgO(001)[^{57}Fe(26Å)/Cr(13Å)]_{20}$

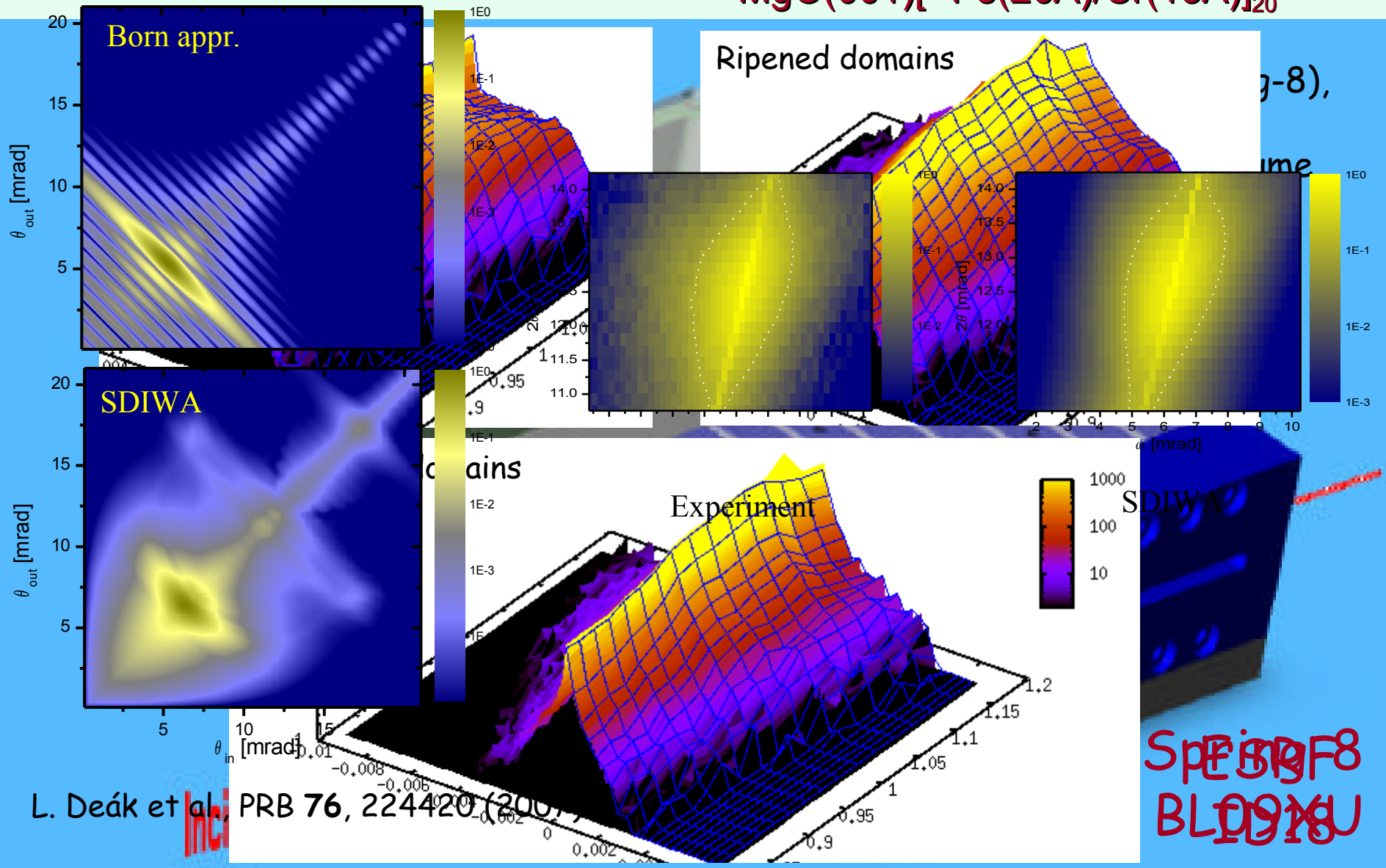

L. Deák et al., PRB **76**, 224420 (2007)

Outlook

- 

ectors for high-field and
experiments
- and synchrotron UHV
- Lateral structures
  - Mössbauer microscopes (laboratory and synchrotron)
  - APD-arrays for diffuse SMR
  - Micro- and nanobeams
- New beamlines (PETRA III)…

Prediction is very difficult, especially about the future (N. Bohr)

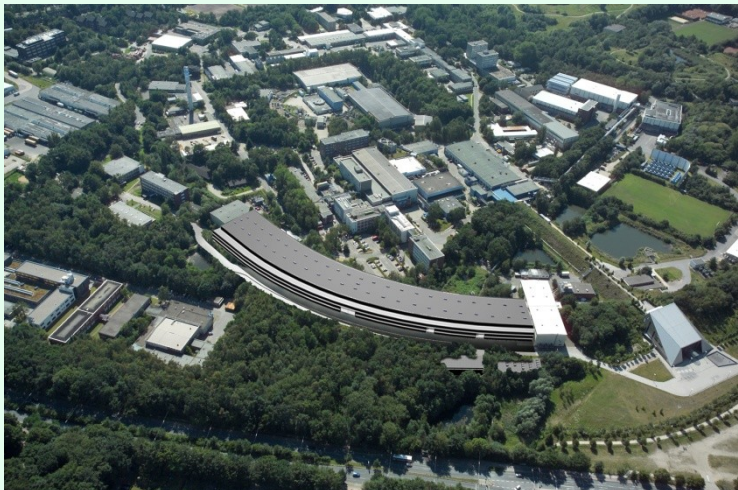

Conclusions

- Mössbauer spectroscopy has recently made a major impact to thin-film magnetism and, conversely, thin-film magnetism has generated a significant development in the methodology of Mössbauer spectroscopy.
- Magnetic thin films may be efficiently studied with Mössbauer spectroscopy both in laboratories and at synchrotrons. The development of these two approaches mutually stimulates each other and, nowadays, a surprisingly wide range of experiments can be performed with laboratory sources.
- Do not hesitate to go to a synchrotron when it is the only way of performing the experiment. But only go to the synchrotron if you are really sure that your experiment cannot be done in the laboratory. Are you sure indeed?

Acknowledgements to:

D. Aernout
L. Bottyán
A.I. Chumakov
B. Croonenborghs
L. Deák
B. Degroote
J. Dekoster
T.H. Deschaux-Beaume
E. Harth
Yu.N. Khaidukov
H.J. Lauter
V. Lauter-Pasyuk
O. Leupold
M. Major
J. Meersschaut
D.G. Merkel
Yu.V. Nikitenko
O. Nikonov
A.V. Petrenko
V.V. Proglyado
R. Rüffer
H. Spiering
C. Strohm
J. Swerts
E. Szilágyi
F. Tanczikó
K. Temst
V. Vanhoof
A. Vantomme
D. Visontai

ESRF Grenoble ILL Grenoble JINR Dubna
KFKI RMKI Budapest KU Leuven University Mainz